Journal of Applied Analysis and Computation
Volume 8, Number 1, February 2018, 379–389
Website:http://jaac-online.com/
DOI:10.11948/2018.379

INFLUENCE OF CROSS DIFFUSIONS ON MIXED CONVECTION CHEMICAL REACTION FLOW IN A VERTICAL CHANNEL WITH NAVIER SLIP: HOMOTOPY APPROACH

K. Kaladhar[1,†] and E. Komuraiah[1]

Abstract This paper is to examine the incompressible, laminar mixed convective Navier slip flow between vertical plates with cross diffusion effects. This research includes the first order chemical reaction also. The resulting equations with boundary conditions are reduced into dimensionless form using appropriate transformations. The series solutions are developed through a modern technique known as the homotopy analysis method. The convergent expressions of velocity components and temperature are derived. The influence of emerging parameters on fluid flow quantities have been presented graphically. Also, the nature of physical quantities are shown in tabular form.

Keywords Soret effect, mixed convection, Dufour effect, chemical reaction, Navier slip, HAM.

MSC(2010) 76E06, 80A32, 76D05, 80A20.

1. Introduction

Combined heat and mass transfer in mixed convection flow between vertical parallel plates has a remarkable significance in various fields. The applications and developments of heat and mass transfer has been addressed by Patil and Chamkha [21]. In view of applications, Sinha and Misra [22] studied the impact of thermophoresis and heat generation on mixed convection hydromagnetic flow with mass transfer over an inclined nonlinear porous shrinking sheet numerically. Recently, Bilal *et al.* [1] presented the thermal radiation effect on MHD mixed convection flow of Jeffrey nanofluid over a radially stretching surface theoretically. Most recently, Mahanthesh *et al.* [18] and Kandasamy *et al.* [12] have been investigated for the importance of heat and mass transfer on various fluids in different geometries.

Generally the no-slip condition has been accepted for the fluid over a solid surface boundary condition. At the solid boundary the general boundary conditions for slip flow has been proposed by Navier [20]. Beg *et al.* [2] presented the early literature and application of the slip flow in various geometries. in view of significance, Mukhopadhyay *et al.* [19] presented the effects of slip flow on MHD mixed convection over a vertical porous plate. Later, Das *et al.* [3] considered the influence of viscous

†Email address:kkr.nitpy@gmail.com(K. Kaladhar)
[1]Department of Mathematics, National Institute of Technology Puducherry, India-609609

dissipation and Joule heating over an inclined porous plate. Most recently, Javed and Mustafa [8] analyzed various characteristics Slip flow on a mixed convection third-grade fluid near the orthogonal stagnation point on a vertical surface.

The Soret and Dufour effects are encountered in many areas for instance chemical engineering, geosciences etc.,. The applications and early literature can be seen in [17]. Recently, Srinivasacharya *et al.* [23] studied the mixed convection flow along a vertical wavy surface with the effects of cross diffusion and variable properties in a porous medium. Hayat *et al.* [7] investigated the effects of chemical reaction, heat source/sink, soret and dufour on three-dimensional flow over an exponentially stretching surface with porous medium. Most recently, Duba *et al.* [4] studies the soret and dufour effects on thermohaline convection in rotating fluids. The importance and past contributions on linear reaction can been in the works of Gireesha and Mahanthesh [5], Kothandapani and Prakash [10] and Gireesha *et al.* [6]. Krupa Lakshmi *et al.* [11] presented the numerical study of the effects of diffusion-thermo and thermo-diffusion on two-phase boundary layer flow past a stretching sheet with fluid-particle suspension and chemical reaction. Most recently, Jawali *et al.* [9] presented the influence of first order chemical reaction in a vertical double passage channel filled with electrically conducting fluid. Sampath Kumar *et al.* [24] studied the nature of the Magnetohydrodynamic flow of williamson Nanofluid due to an exponentially stretching surface in the presence of Thermal Radiation and Chemical Reaction. Mahanthesh *et al.* [16] analyzed the chemical reaction and partial slip effects on the three-dimensional flow of a nanofluid impinging on an exponentially stretching surface.

In this paper, the influence of chemical reaction, cross diffusion effects on mixed convection navier slip flow in a vertical channel has been investigated. The survey clearly exhibits that the slip flow with cross diffusions between vertical parallel plates has not been reported else where. In view of significance, the authors are motivated to take this problem. Homotopy analysis method (HAM) [13–15] has been used for the solution of the present problem. Convergence of the resulting series solution is explained. Then the discussion with respect to the pertinent parameters of the present study on the solutions of velocity, temperature and concentration components.

2. Mathematical Modelling

We consider the two dimensional mixed convection fluid flow with navier slip boundary in a vertical channel. Flow configuration is given below in Fig. 1. All the fluid properties are assumed to be constant with the exclusion that the density in the buoyancy term of the balance of momentum equation. All the parameters are depend on y only since the present study consists of infinitely long plates. The governing two dimensional steady flow equations can be put into the form:

$$\frac{\partial v}{\partial y} = 0 \;\Rightarrow\; v = v_0, \tag{2.1}$$

$$v_0\rho\frac{\partial u}{\partial y} = \rho g\beta_T(T - T_1) + \rho g\beta_C(C - C_1) + \mu\frac{\partial^2 u}{\partial y^2} - \frac{dP}{dx}, \tag{2.2}$$

$$v_0\frac{\partial T}{\partial y} = \alpha\frac{\partial^2 T}{\partial y^2} + \frac{\mu}{\rho C_P}\left(\frac{\partial u}{\partial y}\right)^2 + \frac{DK_T}{C_S C_P}\frac{\partial^2 C}{\partial y^2}, \tag{2.3}$$

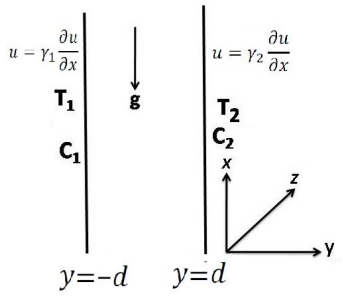

Figure 1. Physical model and coordinate system.

$$v_0 \frac{\partial C}{\partial y} = D \frac{\partial^2 C}{\partial y^2} + \frac{DK_T}{T_m} \frac{\partial^2 T}{\partial y^2} - K_1(C - C_1), \tag{2.4}$$

with

$$y = -d : u = \gamma_1 \frac{\partial u}{\partial y}, \quad T = T_1, \quad C = C_1, \tag{2.5a}$$

$$y = d : u = \gamma_2 \frac{\partial u}{\partial y}, \quad T = T_2, \quad C = C_2, \tag{2.5b}$$

where u and v are the velocities in x and y directions respectively. α is the thermal diffusivity, μ is the viscosity coefficient, β_C is the solutal expansion coefficient, K_T is the thermal conductivity coefficient, T_m is the mean fluid temperature, β_T is the thermal expansion coefficient, g is the acceleration due to gravity, K_1 is the chemical reaction rate, γ_1 and γ_2 are the slip coefficients.

Introducing the following dimensionless parameters

$$\eta = \frac{y}{d}, \;\; u = u_0 f, \;\; \theta = \frac{T - T_1}{T_2 - T_1}, \; \phi = \frac{C - C_1}{C_2 - C_1}, \tag{2.6}$$

we obtain the governing non-dimensional equations from (2.2)–(2.4) as

$$f'' + \frac{Gr_T}{Re}\theta + \frac{Gr_C}{Re}\phi - Rf' - A = 0, \tag{2.7}$$

$$\theta'' - RPr\theta' + Br(f')^2 + PrD_f\phi'' = 0, \tag{2.8}$$

$$\phi'' - RSc\phi' + ScS_r\theta'' - KSc\phi = 0, \tag{2.9}$$

with

$$\begin{aligned} &\eta = -1 : f = \beta_1 f', \; \theta = \phi = 0, \\ &\eta = 1 : f = \beta_2 f' \quad \text{and} \quad \theta - 1 = \phi - 1 = 0, \end{aligned} \tag{2.10}$$

where the primes denote differentiation with respect to η, $R = \frac{\rho v_0 d}{\mu}$ is the suction/injuction parameter, $Gr_T = \frac{\rho^2 g \beta_T d^3}{\mu^2}(T_2 - T_1)$ is the temperature Grashof number, $Re = \frac{v_0 d}{\nu}$ is the Reynolds number, $Gr_C = \frac{\rho^2 g \beta_C d^3}{\mu^2}(C_2 - C_1)$ is the concentration Grashof number, $Pr = \frac{\mu C_p}{K_f}$ is the Prandtl number, $Br = \frac{\mu u_0^2}{K_f(T_2 - T_1)}$ is the Brinkman number, $S_r = \frac{DK_T(T_2 - T_1)}{\nu T_m(C_2 - C_1)}$ is the Soret number, u_0 is the entrance

velocity, $A = \frac{d^2}{\mu u_0}\frac{dP}{dx}$ is the constant pressure gradient, $Sc = \frac{\nu}{D}$ is the Schmidt number, $K = \frac{K_1 d^2}{\nu}$ is the chemical reaction parameter and $D_f = \frac{DK_T(C_2-C_1)}{\nu C_S C_P(T_2-T_1)}$ is the Dufour number. $\beta_1 = \frac{\gamma_1}{d}$, and $\beta_2 = \frac{\gamma_2}{d}$ are the slip parameters.

The skin-friction coefficients(C_f), heat (Nu) and mass (Sh) fluxes at the vertical walls are given by

$$\begin{aligned} ReC_{f_1} = f'(-1),\ ReC_{f_2} = f'(1),\ Nu_{1,2} = -\,\theta'(\eta)|_{\eta=-1,1}\,, \\ Sh_{1,2} = -\,\phi'(\eta)|_{\eta=-1,1}\,, \end{aligned} \tag{2.11}$$

where

$$C_f = \frac{\tau_w}{\rho u_0^2},\ Nu = \frac{q_w d}{K_f(T_2-T_1)},\ Sh = \frac{q_m d}{D(C_2-C_1)}, \tag{2.12}$$

and

$$\begin{aligned} \tau_w = \mu\left.\frac{\partial u}{\partial y}\right|_{y=\pm d};\ q_w = -K_f\left.\frac{\partial T}{\partial y}\right]_{y=\pm d}, \\ q_m = -D\left.\frac{\partial C}{\partial y}\right]_{y=\pm d}. \end{aligned} \tag{2.13}$$

Effect of the various parameters involved in the investigation on physical coefficients are discussed in the following section.

3. Homotopy solution

For Homotopy solutions the initial approximations are chosen as

$$f_0(\eta) = 0, \quad \theta_0(\eta) = \frac{1+\eta}{2}, \quad \phi_0(\eta) = \frac{1+\eta}{2}; \tag{3.1}$$

with the auxiliary linear operator is

$$L_1 = \frac{\partial^2}{\partial \eta^2} \text{ such that } L_1(c_1\eta + c_2) = 0 \tag{3.2}$$

in which c_1 and c_2 are the arbitrary constants. Zeroth-order deformations consists of h_1, h_2 and h_3 (the convergence control parameters).

The zeroth-order deformations, N_1, N_2 and N_3 and the average residual errors of f, θ and ϕ are considered as explained in [13].

h-curves are plotted with $Br = 0.5, S_r = 0.5, Re = 2, Pr = 0.71, R = 2, Sc = 0.22, Gr_T = 10, Gr_C = 10, Gr = 0.5, A = 1, \beta_1 = \beta_2 = 0.1, D_f = 0.5, K = 1$ for the optimal values of h_1, h_2 and h_3 and are presented in Figs 2-4. The admissible values of h_1, h_2 and h_3 are noted as -0.7007, -0.921402, -1.23618 respectively. The average residue errors (as explained in [13]) presented in Figs. 5-7. Lastly, at different order of approximations the total average residual errors are shown in Table 1 also the convergence of the series solutions are expressed in Table 2.

4. Results and Discussion

Figures 8 to 18 represents the nature of velocity ($f(\eta)$), temperature ($\theta(\eta)$) and concentration ($\phi(\eta)$) profiles with various values of the flow parameters. To study

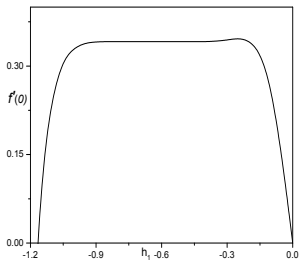

Figure 2. The h curve of $f(\eta)$

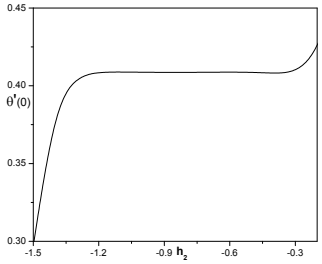

Figure 3. The h curve of $\theta(\eta)$

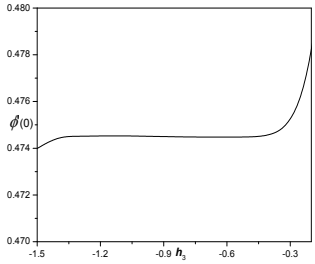

Figure 4. The h curve of $\phi(\eta)$

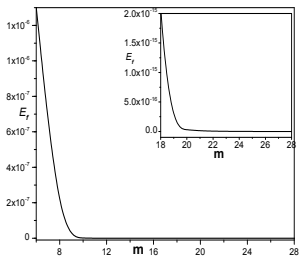

Figure 5. The average residual error of $f(\eta)$

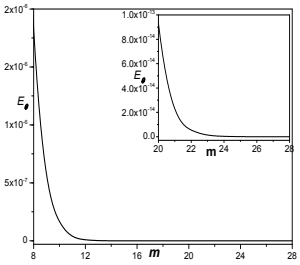

Figure 6. The average residual error of $\theta(\eta)$

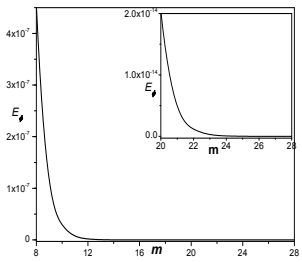

Figure 7. The average residual error of $\phi(\eta)$

Table 1. Total average residual errors at different order of approximations

Order	*Error*
10	5.59×10^{-08}
14	1.74×10^{-10}
16	9.81×10^{-12}
18	5.51×10^{-13}
20	3.21×10^{-14}
26	7.51×10^{-18}
28	4.51×10^{-19}
30	2.62×10^{-20}

Table 2. Convergence of HAM solutions for different order of approximations

Order	$f(0)$	$\theta(0)$	$\phi(0)$
4	0.021776979004782014235	0.38559419324090157963	0.42288916753879661020
8	0.022614477496261448143	0.38717691564797665309	0.42310899278580053604
12	0.022619681332013448304	0.38712609899139193759	0.42310987244234326543
16	0.022618681469241187218	0.38712537512494520966	0.42311091761095034575
20	0.022618722394051123091	0.38712538858396874045	0.42311090033263530454
24	0.022618724100545214329	0.38712539530855802253	0.42311089792529005107
28	0.022618724167709942619	0.38712539549088162011	0.42311089780441071055
30	0.022618724163445169123	0.38712539548575607479	0.42311089780339915364
32	0.022618724162183156892	0.38712539548276981262	0.42311089780323893491

the influence of the flow parameters, the other parameters were fixed at $Re = 2, Pr = 0.71, Sc = 0.22, Br = 1, Gr = 1$.

The effect of the slip flow parameter β_1 on velocity profile is shown in Fig. 8. It can depict from this figure that the velocity profile increases with an increase at the initial wall where as a slight reverse trend is observed at the second plate with an increase in β_1. Figure 9 demonstrates that the influence of β_2 on $f(\eta)$. It is noted from this figure that the velocity profile decreases slightly at the injection plate and increases noticeably at the terminal wall as β_2 increases.

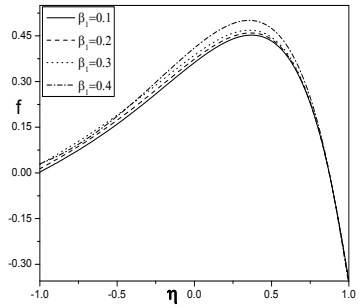

Figure 8. Variation $f(\eta)$ with β_1 when $\beta_2 = 0.1, Sr = 0.5, D_f = 0.5, K = 1.0$

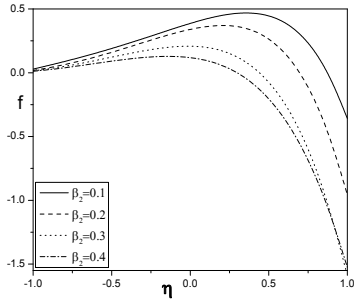

Figure 9. Variation $f(\eta)$ with β_2 when $\beta_1 = 0.1, Sr = 0.5, D_f = 0.5, K = 1.0$

It is noted from figure 10 that as Sr increases the flow velocity increases. This is due to the reason that either decrease in the temperature difference or increase in the concentration difference leads to increase in Sr, with this the lowest peak of the velocity compatible with the lowest soret number. Figure 11 presents the effect of Sr on θ. It is noticed that as Sr increases the temperature profile decreases. Figure 12 shows the effect of Sr on ϕ. It is seen that concentration profile increases as soret parameter increases. This exhibits that the flow field is appreciably influenced with Sr.

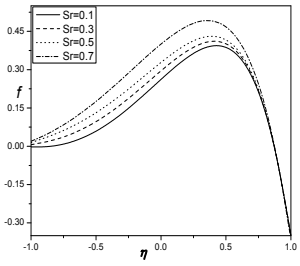

Figure 10. Soret effect on $f(\eta)$ when $\beta_1 = 0.1, \beta_2 = 0.1, D_f = 0.5, K = 1.0$

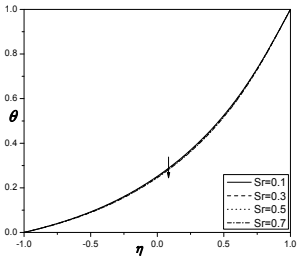

Figure 11. Soret effect on $\theta(\eta)$ when $\beta_1 = 0.1, \beta_2 = 0.1, D_f = 0.5, K = 1.0$

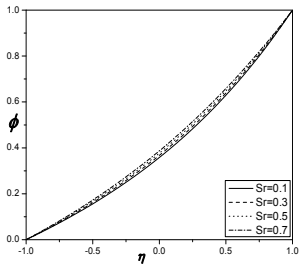

Figure 12. Soret effect on $\phi(\eta)$ when $\beta_1 = 0.1, \beta_2 = 0.1, D_f = 0.5, K = 1.0$

The influence of (D_f) on flow velocity can be noted in figure 13. It is seen from this figure that the $f(\eta)$ increases as D_f increases. When the temperature difference increases or concentration difference decreases leads to the increase in D_f. So, the lowest peak of the flow velocity compatible with the lowest Dufour number. The influence of D_f on temperature profile can be seen in Fig. 14. It is observed that the temperature of the fluid increases as D_f increases. Fig. 15

explains that the dimensionless concentration decreases as D_f increases. This is because of temperature gradients contribution to diffusion of the species.

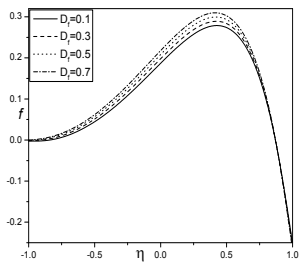

Figure 13. Dufour effect on $f(\eta)$ when $\beta_1 = 0.1, \beta_2 = 0.1, Sr = 0.5, K = 1.0$

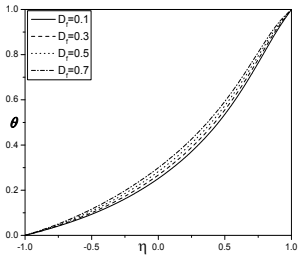

Figure 14. Dufour effect on $\theta(\eta)$ when $\beta_1 = 0.1, \beta_2 = 0.1, Sr = 0.5, K = 1.0$

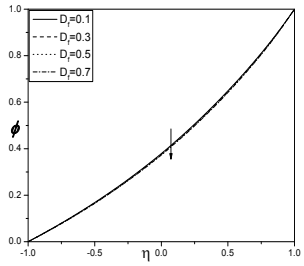

Figure 15. Dufour effect on $\phi(\eta)$ when $\beta_1 = 0.1, \beta_2 = 0.1, Sr = 0.5, K = 1.0$

The influence of K on the flow parameters are shown in figs. 16 to 18. It is noted from figure 16 that the velocity of the fluid decreases as K increases. It is observed that the concentration decreases and temperature profile increases with an increase in reaction parameter K. Since the chemical molecular diffusivity drop down when chemical reaction is high, i.e., lesser diffusion. Hence, they are procured by the transfer of species. The higher K will decrease the concentration species. Therefore with the increase in K suppresses the distribution of the concentration at all the points of the fluid flow.

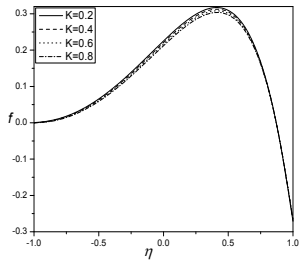

Figure 16. Chemical reaction effect on $f(\eta)$ when $\beta_1 = 0.1, \beta_2 = 0.1, Sr = 0.5, D_f = 0.5$

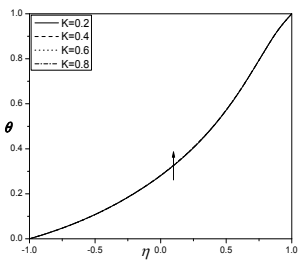

Figure 17. Chemical reaction effect on $\theta(\eta)$ when $\beta_1 = 0.1, \beta_2 = 0.1, Sr = 0.5, D_f = 0.5$

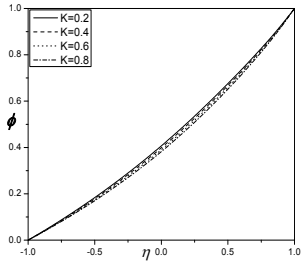

Figure 18. Chemical reaction effect on $\phi(\eta)$ when $\beta_1 = 0.1, \beta_2 = 0.1, Sr = 0.5, D_f = 0.5$

Variation of slip parameters (β_1 and β_2), thermal diffusion parameter (Sr), diffusion thermo parameter (D_f), together with the chemical reaction parameter K are shown in Table 3 by fixing the remaining parameters. It is seen that the friction factor increases at both the walls with an increase in the slip parameters β_1 while the revere trend is noticed with an increase in β_2. It clear that increase in β_1 leads to decrease in heat transfer coefficient at the plates where as the mass transfer rate decreases at the initial wall and increases at the terminal wall. It can be observed that at the initial plate the heat transfer rate increases and at the second plate it is found to be decreases while the reverse trend is perceived on mass transfer rate with an increase in β_2. It is observed from this table that the skin friction coefficient, heat transfer rate increases at the injection wall and decreases at the

terminal wall with the increase of Soret parameter (Sr), where as mass transfer rate have reverse trend at both the plates. It is noticed that higher values of dufour parameter (D_f) increases the friction factor and mass transfer rate at the initial plate and decreases at the suction wall, while heat transfer rate shows the reverse trend at two walls. The effect of chemical reaction parameter K on skin friction, heat and mass transfer rates are presented in Table 3. It is seen from the table that the skin friction coefficient and heat transfer rates are decreases at the injection wall and those are increases at the suction wall with the enhance in K where as we noticed the reverse trend in case of mass transfer rate. It is also seen from this table that the higher values of K increases the mass transfer rate at $\eta = -1$ and decreases at $\eta = 1$. The influence of the emerging parameters are patently obvious from the Table 3 and hence are not discussed for conciseness.

Table 3. Effects of skin friction coefficient, heat and mass transfer rates for various values of Sr, D_f, β_1, β_2 and K

β_1	β_2	Sr	D_f	K	$f'(-1)$	$f'(1)$	Nu_1	Nu_1	Sh_1	Sh_2
0.1	0.1	0.5	0.5	0.5	-0.18856	-0.42812	-0.12984	-1.37688	-0.32103	-0.71900
0.2	0.1	0.5	0.5	0.5	-0.18763	-0.38085	-0.12992	-1.37889	-0.32104	-0.71879
0.3	0.1	0.5	0.5	0.5	-0.18669	-0.33419	-0.13004	-1.37977	-0.32105	-0.71870
0.1	0.1	0.5	0.5	0.5	-0.18856	-0.42812	-0.12984	-1.37688	-0.32103	-0.71900
0.1	0.2	0.5	0.5	0.5	-0.19131	-0.57358	-0.12984	-1.36359	-0.32102	-0.72046
0.1	0.3	0.5	0.5	0.5	-0.19666	-0.87757	-0.13090	-1.30194	-0.32097	-0.72725
0.1	0.1	0.2	0.5	0.5	-0.19104	-0.40981	-0.13236	-1.35170	-0.30258	-0.78158
0.1	0.1	0.4	0.5	0.5	-0.18939	-0.42194	-0.13068	-1.36836	-0.31487	-0.74026
0.1	0.1	0.6	0.5	0.5	-0.18772	-0.43437	-0.12902	-1.38553	-0.32722	-0.69735
0.1	0.1	0.5	0.2	0.5	-0.19170	-0.40310	-0.10959	-1.44422	-0.32260	-0.71121
0.1	0.1	0.5	0.4	0.5	-0.18962	-0.41969	-0.12308	-1.39981	-0.32156	-0.71635
0.1	0.1	0.5	0.6	0.5	-0.18749	-0.43665	-0.13662	-1.35345	-0.32051	-0.72171
0.1	0.1	0.5	0.5	0.2	-0.18661	-0.44241	-0.12819	-1.39506	-0.33461	-0.67409
0.1	0.1	0.5	0.5	0.4	-0.18792	-0.43280	-0.12931	-1.38288	-0.32547	-0.70420
0.1	0.1	0.5	0.5	0.6	-0.18919	-0.42351	-0.13037	-1.37095	-0.31669	-0.73364

5. Conclusions

Two dimensional mixed convection flow in a vertical channel in presence of chemical reaction and the cross diffusion effects with navier slip. Homotopy Analysis Method has been employed to solve the final system of equations. The markable findings are summarized as:

- Flow velocity increases, rate of mass transfer decreases at the injection wall and there is an opposite trend at the suction wall with an increase in β_1.
- As β_1 increases, the heat transfer rate decreases and friction factor increases at both the walls.
- As β_2 increases, the fluid flow velocity and friction factor decreases (slightly at the injection wall and marginally at the suction wall). Where as the heat transfer rate disintegrates at the injection wall and increases at the end wall while the opposite nature is noticed on the rate of mass transfer with an enhance in β_2.

- It is noticed that the velocity and concentration of the fluid increases and temperature profile decreases with an increase in Soret parameter. Also, it is identified that the friction factor, Nusselt number increases at the injection plate and decreases at the end wall as Sr increases, where as mass transfer rate shows the reverse trend at both the walls.
- Fluid flow velocity, θ increases and the dimensionless concentration profile decreases as D_f increases. It is seen that as dufour parameter increases, the skin friction and mass transfer rate increases at $\eta = -1$ and decreases at $\eta = 1$ wall, while the reverse trend is noticed in case of heat transfer rate at both the walls.
- As reaction parameter increases, the velocity and concentration of the fluid decreases and the temperature profile increases. It is also observed that the values of $f'(0)$, Nusselt numbers are decreases at the initial wall and those are increases at the terminal plate where as the reverse trend is observed in case of mass transfer rate with an increase in K.

References

[1] M. B. Ashraf, T. Hayat, A. Alsaedi and S. A. Shehzad, *Convective heat and mass transfer in MHD mixed convection flow of Jeffrey nanofluid over a radially stretching surface with thermal radiation*, J. Cent. South Univ, 2015, 22(3), 1114–1123.

[2] O. A. Bég, M. J. Uddin, M. M. Rashidi and N. Kavyani, *Double-diffusive radiative magnetic mixed convective slip flow with Biot and Richardson number effects*, J. Engin. Thermophys, 2014, 23(2), 79–97.

[3] S. Das, R. N. Jana and O. D. Makinde, *Magnetohydrodynamic mixed convective slip flow over an inclined porous plate with viscous dissipation and Joule heating*, Alexandria Engineering Journal, 2015, 54(2), 251–261.

[4] C. T. Duba, M. Shekar, M. Narayana and P. Sibanda, *Soret and Dufour effects on thermohaline convection in rotating fluids*, Geophysical & Astrophysical Fluid Dynamics, 2016, 110(4), 317–347.

[5] B. J. Gireesha and B. Mahanthesh, *Perturbation solution for radiating viscoelastic fluid flow and heat transfer with convective boundary condition in nonuniform channel with hall current and chemical reaction*, ISRN Thermodynamics, Article ID 935481, 14 pages, 2013. doi:10.1155/2013/935481.

[6] B. J. Gireesha, B. Mahanthesh and M. M. Rashidi, *MHD boundary layer heat and mass transfer of a chemically reacting Casson fluid over a permeable stretching surface with non-uniform heat source/sink*, International Journal of Industrial Mathematics, 2015, 7(3), 247–260.

[7] T. Hayat, T. Muhammad, S. A. Shehzad and A. Alsaedi, *Soret and Dufour effects in three-dimensional flow over an exponentially stretching surface with porous medium, chemical reaction and heat source/sink*, International Journal of Numerical Methods for Heat & Fluid Flow, 2015, 25(4), 762–781.

[8] T. Javed and I. Mustafa, *Slip effects on a mixed convection flow of a third-grade fluid near the orthogonal stagnation point on a vertical surface*, J Appl Mech Tech Phy, 2016, 57(3), 527–536.

[9] C. Jawali, J. Umavathi, Prathap Kumar and Mikhail A. Sheremet, *Heat and mass transfer in a vertical double passage channel filled with electrically conducting fluid*, Physica A: Statistical Mechanics and its Applications, 2017, 465(1),195–216.

[10] M. Kothandapani and J. Prakash, *Effects of thermal radiation and chemical reactions on peristaltic flow of a Newtonian nanofluid under inclined magnetic field in a generalized vertical channel using homotopy perturbation method*, Asia-Pac. J. Chem. Eng., 2015, 10(2), 259–272.

[11] K. L. Krupa Lakshmi, B. J. Gireesha, Rama. S. R. Gorla and B. Mahanthesh, *Effects of diffusion-thermo and thermo-diffusion on two-phase boundary layer flow past a stretching sheet with fluid-particle suspension and chemical reaction: A numerical study*, Journal of the Nigerian Mathematical Society, 2016, 35(1), 66–81.

[12] R. Kandasamy, C. Jeyabalan and K. K. Sivagnana Prabhu, *Nanoparticle volume fraction with heat and mass transfer on MHD mixed convection flow in a nanofluid in the presence of thermo-diffusion under convective boundary condition*, Appl Nanosci, 2016, 6(2), 287–300.

[13] K. Kaladhar and D. Srinivasacharya, *Combined effects of hall, joule heating and thermal diffusion on mixed convection flow in a vertical channel saturated with couple stress fluid*, Frontiers in Heat and Mass Transfer, 2016, 7(6), 1–10.

[14] S. Liao, *Beyond perturbation. Introduction to homotopy analysis method*. Chapman and Hall/CRC Press, Boca Raton, 2003.

[15] S. Liao, *An optimal homotopy-analysis approach for strongly nonlinear differential equations*, Commun. Nonlinear Sci.Numer. Simul, 2010, 15(8), 2003–2016.

[16] B. Mahanthesh, F. Mabood and B. J. Gireesha, *Effects of chemical reaction and partial slip on the three-dimensional flow of a nanofluid impinging on an exponentially stretching surface*, Eur. Phys. J. Plus, 2017, 132, 113–130.

[17] M. A. A. Mahmoud and A. M. Megahed, *Thermal radiation effect on mixed convection heat and mass transfer of a non-Newtonian fluid over a vertical surface embedded in a porous medium in the presence of thermal diffusion and diffusion-thermo effects*, J. Appl. Mech. Tech. Phys, 2013, 54(1), 90–99.

[18] B. Mahanthesh, B. J. Gireesha and Rama Subba Reddy Gorla, *Heat and mass transfer effects on the mixed convective flow of chemically reacting nanofluid past a moving/stationary vertical plate*, Alexandria Engineering Journal, 2016, 55(1), 569–581.

[19] S. Mukhopadhyay and I. Chandra Mandal, *Magnetohydrodynamic (MHD) mixed convection slip flow and heat transfer over a vertical porous plate*, Engineering Science and Technology, an International Journal, 2015, 18(1), 98–105.

[20] C. L. M. H. Navier, *Memoire sur les lois du mouvement des fluides*, Mem Acad R Sci Paris, 1823, 6, 389–416.

[21] P. M. Patil and A. J. Chamkha, *Heat and mass transfer from mixed convection flow of polar fluid along a plate in porous media with chemical reaction*, Int J of Numerical Methods for Heat & Fluid Flow, 2013, 23(5), 899–926.

[22] A. Sinha and J. C. Misra, *Mixed Convection Hydromagnetic Flow with Heat Generation, Thermophoresis and Mass Transfer over an Inclined Nonlinear*

Porous Shrinking Sheet: A Numerical Approach, Journal of Mechanics, 2014, 30(5), 491–503.

[23] D. Srinivasacharya, B. Mallikarjuna and R. Bhuvanavijaya, *Soret and Dufour effects on mixed convection along a vertical wavy surface in a porous medium with variable properties*, Ain Shams Eng. J, 2015, 6(2), 553–564.

[24] P. B. Sampath Kumar, B. J. Gireesha, R. S. R. Gorla and B. Mahanthesh, *Magnetohydrodynamic Flow of Williamson Nanofluid Due to an Exponentially Stretching Surface in the Presence of Thermal Radiation and Chemical Reaction*, Journal of Nanofluids, 2017, 6(2), 264–272.